

Reaction of the Cationic Cluster [Os₃(μ-H)(CO)₁₀(μ-η¹:η²-=C=C=CMe₂)]BF₄ with Triphenylphosphine. Formation and Transformations of the σ-Acetylide Cluster [Os₃(μ-H)(CO)₁₀(PPh₃)(σ-C≡CCMe₂PPh₃)]BF₄ and Two Isomeric Clusters [Os₃(μ-H)(CO)₉(PPh₃)(μ-σ:η²-C≡CCMe₂PPh₃)]BF₄

Ol'ga A. Kizas,* Vasily V. Krivykh, Evgenii V. Vorontsov, Oleg L. Tok,
Fedor M. Dolgushin, and Avthandil A. Koridze*

A. N. Nesmeyanov Institute of Organoelement Compounds, Russian Academy of Science,
Vavilova 28, 119991 Moscow, Russian Federation

Received February 21, 2001

The complex [Os₃(μ-H)(CO)₁₀(μ-η¹:η²-=C=C=CMe₂)]BF₄ (**1**) reacts with PPh₃ at -78 °C to give isomeric phosphonium derivatives of the formula [Os₃(μ-H)(CO)₁₀(μ-σ:η²-C≡CCMe₂PPh₃)]BF₄ (**2** and **3**); the isomerization **2** → **3** takes place. The second PPh₃ molecule attacks **3** at the metal atom, substituting a CO in the Os(CO)₄ unit to form the cluster [Os₃(μ-H)(CO)₉(PPh₃)(μ-σ:η²-C≡CCMe₂PPh₃)]BF₄ (**4**), which further transforms to the acetylide σ-complex [Os₃(μ-H)(CO)₁₀(PPh₃)(σ-C≡CCMe₂PPh₃)]BF₄ (**5**). The latter decarbonylates in the temperature range 25–55 °C to yield the cluster [Os₃(μ-H)(CO)₉(PPh₃)(μ-σ:η²-C≡CCMe₂PPh₃)]BF₄ (**6**), which is isomeric with **4**. Complex **5** is considered to be an intermediate in the isomerization of the clusters [Os₃(μ-H)(CO)₉(PPh₃)(μ-σ:η²-C≡CCMe₂PPh₃)]BF₄ (**4**, **6**). Clusters **2**–**6** have been characterized by their ¹H, ³¹P, and ¹³C NMR spectra, and X-ray structural analyses have been performed for complexes **5** and **6**.

Introduction

The carbon atoms of acetylide ligands are known to gain carbocationic character in clusters.¹ For this reason, acetylide clusters, particularly osmium clusters, react readily with neutral P,^{2a} N,^{2b–d} O,^{2c,e} and C nucleophiles.^{2f} Formation of cationic complexes is known to increase the electrophilic character of the ligand, thus permitting an extension of the number of nucleophilic reagents. This approach is widely used for mononuclear compounds;³ however, cationic clusters have not been studied as much as their neutral analogues. Earlier we synthesized osmium cationic clusters with various propargyl ligands⁴ and studied their properties: in particular, reactions with triphenylphosphine. We reported the formation of the cationic complex [Os₃(μ-H)(CO)₁₀(μ-η¹:η²-=C=C=CMe₂)]BF₄ (**1**) by protonation of Os₃(μ-H)(CO)₁₀(μ-σ:η²-C≡CCMe₂OMe).⁵ The reaction of **1** with H₂O as a nucleophile led to decarbonylation of the

metal carbonyl fragment to form the neutral cluster Os₃(μ-H)(CO)₉(μ₃-σ:η²: η²-C≡CCMe₂H). Now we report the reaction of **1** with PPh₃.

Experimental Section

The reactions were carried out under an argon atmosphere. All solvents were purified by distillation under dry argon from the appropriate drying agent. NMR spectra were recorded on a Bruker AMX-400 spectrometer at 400.13 MHz for ¹H (relative to Me₄Si), at 161.92 MHz for ³¹P (relative to 85% H₃PO₄) in CD₂Cl₂, and at 100.13 MHz for ¹³C in CD₂Cl₂ and CD₃NO₂ (relative to Me₄Si). The ¹H and ³¹P NMR spectral data are presented in Table 1; the ¹³C NMR spectra are given in Tables 2 and 3.

(3) (a) Krivykh, V. V.; Taits, E. S.; Petrovskii, P. V.; Rybinskaya, M. I. *Metalloorg. Khim.* **1989**, *2*, 939; *Organomet. Chem. USSR (Engl. Transl.)* **1989**, *2*. (b) Krivykh, V. V.; Taits, E. S.; Petrovskii, P. V.; Struchkov, Yu. T.; Yanovsky, A. I. *Mendeleev Commun.* **1991**, *103*. (c) Krivykh, V. V. *Metalloorg. Khim.* **1992**, *5*, 213; *Organomet. Chem. USSR (Engl. Transl.)* **1992**, *5*, 113. (d) Taits, E. S.; Petrovskii, P. V.; Krivykh, V. V. *Izv. Akad. Nauk, Ser. Khim.* **1999**, *1796*; *Russ. Chem. Bull. (Engl. Transl.)* **1999**, *48*, 1774. (e) Casey, C. P.; Yi, C. S. *J. Am. Chem. Soc.* **1992**, *114*, 6597. (f) Blosser, P. W.; Schimpff, D. G.; Gallucci, J. C.; Wojcicki, A. *Organometallics* **1993**, *12*, 1993. (g) Blosser, P. W.; Gallucci, J. C.; Wojcicki, A. *J. Am. Chem. Soc.* **1993**, *115*, 2994. (h) Huang, T.-M.; Chen, J.-T.; Lee, G.-N.; Wang, Y. *J. Am. Chem. Soc.* **1993**, *115*, 1170. (i) Stang, P. J.; Critte, C. M.; Arif, A. M. *Organometallics* **1993**, *12*, 4799. (j) Ogoshi, S.; Tsutsumi, K.; Kurosawa, H. *J. Organomet. Chem.* **1995**, *493*, C19. (k) Wojcicki, A. *New J. Chem.* **1997**, *21*, 733. (l) Chen, J.-T. *Coord. Chem. Rev.* **1999**, *190*–192, 1143.

(4) Krivykh, V. V.; Kizas, O. A.; Vorontsov, E. V.; Dolgushin, F. M.; Yanovsky, A. I.; Struchkov, Yu. T.; Koridze, A. A. *J. Organomet. Chem.* **1996**, *508*, 39.

(5) Krivykh, V. V.; Kizas, O. A.; Vorontsov, E. V.; Koridze, A. A. *Izv. Akad. Nauk, Ser. Khim.* **1996**, *2990*; *Russ. Chem. Bull. (Engl. Transl.)* **1996**, *45*, 2840.

Table 1. ^1H and ^{31}P NMR Data for the Clusters 1–6

cluster	^1H chem shift ^a (δ , ppm)	coupling const (Hz)		^{31}P chem shift ^a (δ , ppm)
		$J(\text{HP})$	$J(^{187}\text{Os}^{-1}\text{H})$	
1	2.6 s (Me)			
	2.2 s (Me)			
	−19.8 s (μ -H)			
2	1.9 d (Me)	17.6		35.6 (P^+)
	1.8 d (Me)	16.4		
	−19.2 s (μ -H)			
3	1.9 d (2Me)	16.8		37.2 (P^+)
	−16.79 s (μ -H)			
4	1.7 d (Me)	20.2		30.5 (P^+)
	1.4 d (Me)	20.0		1.5 (PPh_3)
	−18.2 d (μ -H)	12.6		
5	1.6 d (Me)	17.3		33.7 (P^+)
	1.5 d (Me)	17.6		−0.8 (PPh_3)
	−18.5 dd (μ -H)	11.8, 1.9	39.9 43.8	
6	1.8 d (Me)	16.8		34.9 (P^+) ^b
	1.3 d (Me)	16.4		−2.42 (PPh_3) ^b
	−18.6 d (μ -H)	12.4	45.4 41.8	

^a CD_2Cl_2 . ^b CD_3NO_2 .

Preparation of $[\text{Os}_3(\mu\text{-H})(\text{CO})_{10}(\mu\text{-}\sigma\text{-}\eta^2\text{-C}\equiv\text{CCMe}_2\text{PPh}_3)]\text{BF}_4$ (3). Several drops of a solution of $\text{HBF}_4\text{-Et}_2\text{O}$ in CD_2Cl_2 were added to a solution of $\text{Os}_3(\mu\text{-H})(\text{CO})_{10}(\mu\text{-}\sigma\text{-}\eta^2\text{-C}\equiv\text{CCMe}_2\text{OMe})$ (60 mg, 0.062 mmol, NMR tube) in CD_2Cl_2 at −78 °C. The reaction was monitored by ^1H NMR. Then PPh_3 (114 mg, 0.43 mmol) was added at −78 °C. Complete protonation and formation of **1** usually occurs with a 5-fold excess of the acid, which is why a 7-fold excess of phosphine was used for the reaction. The solution was warmed to room temperature, and diethyl ether was added to the reaction mixture until white crystals of $[\text{HPPh}_3]\text{BF}_4$ precipitated. The solvent was removed in vacuo, the residue was dissolved in the minimum of CH_2Cl_2 , then Et_2O was added until the solution became slightly turbid, and the mixture was kept at 0 °C for several hours. Compound **3** precipitated as dark yellow crystals. The solvent was decanted, and the crystals were dried in vacuo to give **3** (61.6 mg, 78%). Anal. Calcd for $\text{C}_{33}\text{H}_{22}\text{BF}_4\text{O}_{10}\text{Os}_3$: C, 31.28; H, 1.75; F, 5.99; P, 2.44. Found: C, 30.79; H, 1.80; F, 5.83; P, 2.46.

Preparation of $[\text{Os}_3(\mu\text{-H})(\text{CO})_{10}(\text{PPh}_3)(\sigma\text{-C}\equiv\text{CCMe}_2\text{PPh}_3)]\text{BF}_4$ (5). A solution of $\text{HBF}_4\text{-Et}_2\text{O}$ in CD_2Cl_2 was added to a solution of $\text{Os}_3(\mu\text{-H})(\text{CO})_{10}(\mu\text{-}\sigma\text{-}\eta^2\text{-C}\equiv\text{CCMe}_2\text{OMe})$ (25 mg, 0.026 mmol) in CD_2Cl_2 . The protonation conditions were similar to those described for the formation of **3**. PPh_3 (50 mg, 0.19 mmol) was added to the cationic complex **1** obtained. The tube was kept at 0 °C for 48 h and then at room temperature for another 48 h. The ^1H NMR spectrum indicated the presence of complexes **5** and **6** in a 9:1 ratio. Et_2O was added to the reaction mixture until white crystals of $[\text{HPPh}_3]\text{BF}_4$ fully precipitated. The solution was filtered and evaporated, and the residue was dissolved in the minimum amount of CH_2Cl_2 . Then Et_2O was added until the solution became slightly turbid, and the mixture was kept at 0 °C for 1 h. Compound **5** precipitated as bright yellow crystals. The solvent was decanted, and the crystals were dried in vacuo to give **5** (24 mg, 60%). Anal. Calcd for $\text{C}_{51}\text{H}_{37}\text{BF}_4\text{O}_{10}\text{Os}_3\text{P}_2$: C, 40.05; H, 2.44; F, 4.96.; P, 4.05. Found: C, 39.51; H, 2.49; F, 4.47; P, 3.91.

Thermolysis of $[\text{Os}_3(\mu\text{-H})(\text{CO})_{10}(\text{PPh}_3)(\sigma\text{-C}\equiv\text{CCMe}_2\text{PPh}_3)]\text{BF}_4$ (5). A solution of **5** (30 mg, 0.02 mmol) in CD_3NO_2 was heated in a sealed tube at 55 °C for 15 h. The reaction was monitored by ^1H NMR. When the solution contained a 1:1 ratio of **5** to **6**, the tube was opened and treated as described in the previous section. Dark yellow crystals of **6** (14.6 mg, 50%) precipitated.

X-ray Diffraction Study. Details of crystal data and data collection and structure refinement parameters for complexes

5 and **6** are given in Table 4. The structures were solved by direct methods and refined by the full-matrix least-squares technique against F^2 with anisotropic temperature factors for all non-hydrogen atoms. All phenyl rings in structure **5** were refined as rigid fragments with the fixed values of the C–C distances (1.390 Å). The bridging hydride atoms were located in difference syntheses and taken into account as fixed contributions during refinement. The other hydrogen atoms in structures **5** and **6** were placed geometrically and included in the structure factor calculation in the riding model approximation. Data reduction and further calculations were performed using SHELXTL PLUS 5⁶ (for **5**) and SAINT⁷ and SHELXTL-97⁸ (for **6**) on an IBM PC AT computer.

Results and Discussion

Reaction of $[\text{Os}_3(\mu\text{-H})(\text{CO})_{10}(\mu\text{-}\sigma\text{-}\eta^2\text{-C}\equiv\text{CCMe}_2)]\text{BF}_4$ (1) with PPh_3 . When excess PPh_3 is added to a solution of **1** in CD_2Cl_2 at −78 °C, a new set of signals associated with **2** appears in the ^1H NMR spectrum (Table 1). The signal for the hydride ligand is shifted downfield 0.6 ppm compared to that for **1**; the non-equivalent methyl groups give rise to doublets with $J_{\text{H}-\text{P}} = 17.6$ and 16.4 Hz. There is also a low-field signal at δ 9.1 with $J_{\text{H}-\text{P}} = 529$ Hz corresponding to $[\text{HPPh}_3]\text{BF}_4$. In the ^{31}P NMR spectrum there are the signals for the phosphonium phosphorus atom (Table 1); the signals at δ 5.88 and δ −5.6 correspond to $[\text{HPPh}_3]\text{BF}_4$ and PPh_3 , respectively. Thus, the spectral data indicate that the phosphine is attached to the C_γ atom of the hydrocarbon ligand. The ^{13}C NMR spectrum of **2** showed 80% isomerization to **3** during the acquisition time (4 h, at −90 °C); however, signals due to **2** were also observed (Table 2).

The chemical shift for the hydride ligand of **3** (Table 1) corresponds to those for clusters in which the σ,π -acetylidyne and hydride ligands are bridges between the same osmium atoms.^{5,10} The methyl groups of **3** are observed as doublets, with the $J_{\text{H}-\text{P}}$ value indicating the attachment of PPh_3 to the C_γ atom of the hydrocarbon ligand. This is in accord with the ^{31}P spectrum that shows the resonance for the phosphonium phosphorus atom (Table 1). In the hydrocarbon region of the ^{13}C NMR spectrum of cluster **3** (Table 2), there are a singlet and two doublets associated with the α -, β -, and γ -carbon atoms of the hydrocarbon ligand, respectively, and a singlet for the methyl groups. Thus, the spectral data provide evidence that **3** is an acetylidyne cluster with the formula $[\text{Os}_3(\mu\text{-H})(\text{CO})_{10}(\mu\text{-}\sigma\text{-}\eta^2\text{-C}\equiv\text{CCMe}_2\text{PPh}_3)]\text{BF}_4$ (Chart 1).

The equivalency of the Me groups in the ^1H and ^{13}C NMR spectra suggests that **3** is stereochemically non-rigid due to $\sigma,\pi \leftrightarrow \pi,\sigma$ interexchange, as was found earlier for the related cluster $\text{Os}_3(\mu\text{-H})(\text{CO})_{10}(\mu\text{-}\sigma\text{-}\eta^2\text{-C}\equiv\text{CPh})$ (**8**).¹¹ This is confirmed by the ^{13}C NMR spectrum in the carbonyl region (Table 2), in which six sig-

(6) Sheldrick, G. M. *SHELXTL Version 5, Software Reference Manual*; Siemens Industrial Automation: Madison, WI, 1994.

(7) SMART V5.051 and SAINT V5.00, Area Detector Control and Integration Software; Bruker AXS Inc., Madison, WI 53719, 1998.

(8) Sheldrick, G. M. *SHELXTL-97 V5.10*; Bruker AXS Inc., Madison, WI 53719, 1997.

(9) Walker, N.; Stuart, D. *Acta Crystallogr., Sect. A* **1983**, *A39*, 158.

(10) Deemings, A. J.; Hasso, S.; Underhill, M. *J. Chem. Soc., Dalton Trans.* **1975**, 1614.

(11) Kordzhe, A. A.; Kizas, O. A.; Kolobova, N. E.; Petrovskii, P. V. *Izv. Akad. Nauk SSSR, Ser. Khim.* **1984**, 472; *Bull. Acad. Sci. USSR, Div. Chem. Sci. (Engl. Transl.)* **1984**, 33, 437.

Table 2. ^{13}C NMR Data for the Two Isomers of the Cluster $[(\mu\text{-H})\text{Os}_3(\text{CO})_{10}(\mu\text{-}\sigma\text{-}\eta^2\text{-C}\equiv\text{CCMe}_2\text{PPh}_3)]\text{BF}_4$ (2,^a 3)

cluster 2				cluster 3			
signal	^{13}C chem shift (δ , ppm)	coupling const (Hz)		signal	^{13}C chem shift (δ , ppm)	coupling const (Hz)	
		$J(\text{C-P})$	$J(\text{C-H})$			$J(\text{C-P})$	$J(\text{C-H})$
4 (5)	184.7		6.6	V (VI)	181.0		
5 (4)	184.5		9.49	VI (V)	168.9		
2	183.9			II (II')	168.3		w
9	182.4			IV(IV')	92.85		
1	176.1			I (I')	179.5		w
6 (3)	175.3		14.2	III (III')	174.6		w
3 (6)	174.5		~1.5	VII	171.7		
7	173.4		w	VIII	78.1	4.5	
8	170.6			IX	37.5	44.2	
10	170.1			X, XI	26.1		
11	107.2						
12	76.3		11.0				
13	32.4		47.1				
14 (15)	28.8						
15 (14)	26.4						

^a Conditions: -90°C , CD_2Cl_2 .**Table 3.** ^{13}C NMR Data^a for the Clusters $[(\mu\text{-H})\text{Os}_3(\text{CO})_{10}\text{PPh}_3(\sigma\text{-C}\equiv\text{CCMe}_2\text{PPh}_3)]\text{BF}_4$ (5) and $[(\mu\text{-H})\text{Os}_3(\text{CO})_9\text{PPh}_3(\mu\text{-}\sigma\text{-}\eta^2\text{-C}\equiv\text{CCMe}_2\text{PPh}_3)]\text{BF}_4$ (6)

cluster 5				cluster 6			
signal	^{13}C chem shift (δ , ppm)	coupling const (Hz)		signal	^{13}C chem shift (δ , ppm)	coupling const (Hz)	
		$J(\text{C-P})$	$J(\text{C-H})$			$J(\text{C-P})$	$J(\text{C-H})$
3	170.0	w	~11	V	186.1	6.2	
2	170.4		w	IX	185.2	w	
9, 10	170.9			VI	183.0	6.6	~2.6
6	170.5	6.2		III	176.1		3.3
1	175.2		~4.5	VII	175.8	w	
8	183.1	w		I	175.2		4.8
7	183.6			II	171.1		2.8
5	184.2	10.9		VIII	170.6	2.5	
4	184.3	7.6		IV	167.8	5.7	2.5
11 (12)	111.0	6.0		X (XI)	107.8	8.1	5
12 (11)	80.4	11.1		XI (X)	92.5		
13	36.3	48.3	3.8	XII	39.7	41.3	
14	28.6		130	XIII	30.9		130
15	27.4		130	XIV	24.2		130

^a Conditions: -40°C , CD_2Cl_2 .

nals with relative intensities of 1:1:2:2:2:2 are observed for the CO groups. Thus, signals for eight of 10 carbonyl groups are pairwise exchange-averaged.¹¹ Three of four signals with a relative intensity of 2 are markedly broadened due to residual coupling to the hydride. The comparison of the ^{13}C NMR spectra of **3** and **8**¹¹ shows that the broadened signals for **3** have chemical shifts close to those for the CO groups of **8**, which are coupled to the bridging hydride. The signals V and VI of intensity 1 which are not exchange-averaged are assigned to the axial ligands of the $\text{Os}(\text{CO})_4$ unit. The broadest signal is assigned to the CO groups I and I' located trans to the hydride ligand, another two broadened signals might be attributable to the carbonyl groups II, II' and III, III', and finally the nonbroadened signals IV and IV' are assigned to the equatorial ligands of the $\text{Os}(\text{CO})_4$ moiety. The exchange process in **3** could not be frozen out at -90°C as it was for **8**.¹¹

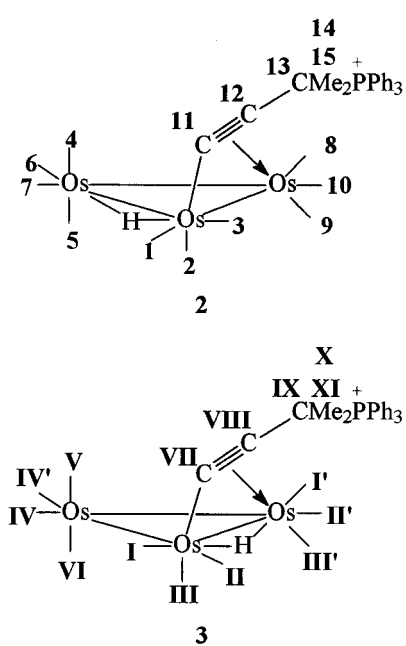
The ^1H and ^{31}P NMR spectra suggest that isomer **2** has a σ, π -acetylidyne ligand. In contrast to **3**, however, the organic ligand is not apparently bridging the $\text{Os}(\mu\text{-H})\text{Os}$ edge, because the chemical shift for the hydride ligand differs from those for **3** and related complexes. Moreover, the Me groups of **2** in the ^1H NMR spectrum are nonequivalent. The spectral data fit the structure

shown in Chart 1. The transformation **1** \rightarrow **2** \rightarrow **3** is shown in Scheme 1. It cannot be ruled out that this transformation may involve hydride migration. In the carbonyl region of the ^{13}C NMR spectrum of the mixture of **2** and **3**, there are 10 signals attributable to **2** (Table 2). The two low-field signals 4 and 5 are assigned to the axial groups of the $\text{Os}(\text{CO})_4(\mu\text{-H})$ unit, and the resonances 3, 6, and 7 are coupled to the hydride and therefore assigned to the equatorial ligands at the $\text{Os}(\mu\text{-H})\text{Os}$ edge. The $J_{\text{C-H}}$ value indicate that the signals 3 and 6 correspond to the CO groups trans to the hydrogen ligand. The low-field signals 2 and 9 can be assigned to the equatorial CO groups on the Os(1) and Os(3) atoms. The highest field signals 8 and 10 are most probably due to the equatorial CO groups on the Os(3) atom. Thus the ^{13}C NMR spectrum of **2** is consistent with the structure with the $\mu\text{-H}$ ligand bound to $\text{Os}(\text{CO})_4$. In this case the $\sigma, \pi \leftrightarrow \pi, \sigma$ rearrangement cannot result in averaging the methyl and carbonyl resonances in the ^1H and ^{13}C NMR spectra, unlike the case for **3**. Our conclusions on the structure of complex **2** are in accord with the data for the isomeric vinyl clusters $\text{Os}_3(\mu\text{-H})(\text{CO})_9(\text{PPh}_3)(\mu\text{-}\sigma\text{-}\eta^2\text{-CH=CH}_2)$.¹² The authors¹² explained interconversion of vinyl isomers by $\sigma, \pi \leftrightarrow \pi, \sigma$ interexchange of the hydrocarbon ligand combined with

Table 4. Crystal Data and Data Collection and Structure Refinement Parameters for 5 and 6

	5	6
formula	$[\text{C}_{51}\text{H}_{37}\text{O}_{10}\text{Os}_3\text{P}_2]\text{BF}_4 \cdot \frac{1}{4}\text{CH}_2\text{Cl}_2$	$[\text{C}_{50}\text{H}_{37}\text{O}_9\text{Os}_3\text{P}_2]\text{BF}_4 \cdot \frac{1}{4}\text{CH}_2\text{Cl}_2$
mol wt	1550.39	1522.38
cryst habit	prism	hexagonal plate
cryst dimens, mm	0.4 × 0.3 × 0.2	0.40 × 0.35 × 0.05
cryst syst	monoclinic	triclinic
space group	$\text{C}2/c$	$\text{P}1$
$a, \text{\AA}$	42.495(9)	14.423(5)
$b, \text{\AA}$	10.377(3)	17.893(6)
$c, \text{\AA}$	25.486(6)	19.415(7)
α (deg)		96.610(7)
β (deg)	108.99(2)	101.782(6)
γ (deg)		90.697(6)
$V, \text{\AA}^3$	10627(4)	4869(3)
Z	8	4
$d(\text{calcd}), \text{g cm}^{-3}$	1.938	2.077
$\mu(\text{Mo Ka}), \text{cm}^{-1}$	73.11	79.74
diffractometer	Siemens P3/PC	SMART 1000 CCD
temp, K	293(2)	110.0(2)
scan mode	$\theta/2\theta$	ω
θ_{max} (deg)	25	25
abs cor	DIFABS [4]	SADABS
transmiss factors, min/max	0.784/1.420	0.579/0.928
no. of collected rflns	10 556	38 940
no. of unique rflns	9336 (0.0819)	17167 (0.0731)
(R_{int})		
no. of obsd rflns	5708	9688
$(I > 2\sigma(I))$		
$R1$ (on F for obsd rflns) ^a	0.0552	0.0561
$wR2$ (on F^2 for all rflns) ^b	0.1271	0.1525

^a $R1 = \sum ||F_0| - |F_c|| / \sum (F_0)$. ^b $wR2 = \{\sum [w(F_0^2 - F_c^2)^2] / \sum w(F_0^2)^2\}^{1/2}$.

Chart 1

the migration of carbonyl groups. We find the transformation of **1** to **3** via **2** somewhat unusual, since direct formation of **3** from **1** seems mechanistically more simple.

Reaction of $[\text{Os}_3(\mu\text{-H})(\text{CO})_{10}(\mu\text{-}\sigma\text{-}\eta^2\text{-C}\equiv\text{CCMe}_2\text{PPh}_3)]\text{BF}_4$ (3) with PPh_3 . Complex **3** reacts with PPh_3

(12) Koike, M.; Hamilton, D. H.; Wilson, S. R.; Shapley, J. R. *Organometallics* **1996**, *15*, 4930.

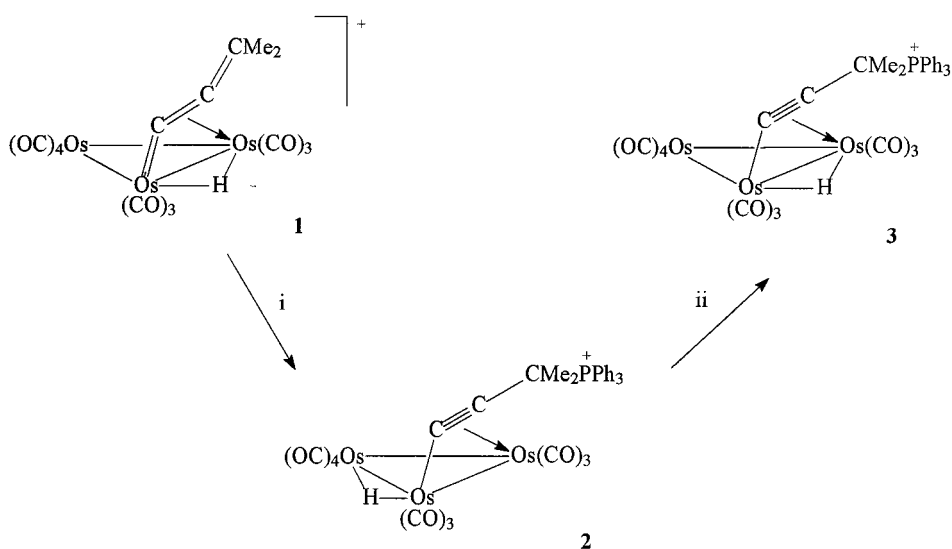
at 0 °C both in the individual state and in situ to form **4**, which transforms rapidly to **5** (Scheme 2). The reaction was monitored by ^1H and ^{31}P NMR. Complex **4** shows in the ^1H NMR spectrum a doublet for the hydride ligand and two doublets associated with the nonequivalent Me groups; $J_{\text{P}-\text{H}}$ values indicate the presence of a phosphonium substituent at the C_γ atom of the hydrocarbon ligand. Complex **5** shows a doublet of doublets for the hydride ligand and two doublets for the Me groups. The ^{31}P NMR spectrum of **5** contains two signals due to the phosphonium substituent and the phosphine ligand (Table 1). The ^{13}C NMR spectrum of **5** recorded at -40 °C displays nine carbonyl resonances (Table 3). The chemical shifts of the two low-field signals 7 and 8 are typical of the axial CO ligands of the $\text{Os}(\text{CO})_4$ unit and can be assigned to these ligands. The low-field signals 4 and 5 with large $J_{\text{C}-\text{P}}$ values are assigned to the axial carbonyl groups of the $\text{Os}(\text{CO})_3\text{PPh}_3$ unit. Signal 6 with a smaller $J_{\text{C}-\text{P}}$ value is assigned to the equatorial group of this fragment. The resonances 1–3 are coupled to the hydride and might be attributable to the CO groups of the $\text{Os}(\text{CO})_3$ unit. Signal 3 with the largest $J_{\text{C}-\text{H}}$ value presumably belongs to the CO group located in a position trans to the hydride. In a temperature range of -40 to +40 °C these resonances gradually broaden and finally coalesce to one broad signal. In the high-field region of the spectrum, there are three doublets (11–13) due to the hydrocarbon ligand. An X-ray analysis established that complex **5** is the phosphine cluster $[\text{Os}_3(\mu\text{-H})(\text{CO})_{10}(\text{PPh}_3)(\sigma\text{-C}\equiv\text{CCMe}_2\text{PPh}_3)]\text{BF}_4$ with a σ -bound phosphonium acetylide ligand. The only example of a stable σ -acetylidyne trinuclear cluster, $\text{Os}_3(\text{CO})_6(\mu\text{-}\eta^2\text{-C}\equiv\text{CPh})(\eta^1\text{-C}\equiv\text{CPh})(\mu\text{-PPh}_2)_2(\text{NH}_2\text{-Et})_2$ (**9**), has been previously reported.¹³

Crystal Structure of $[\text{Os}_3(\mu\text{-H})(\text{CO})_{10}(\text{PPh}_3)(\sigma\text{-C}\equiv\text{CCMe}_2\text{PPh}_3)]\text{BF}_4$ (5). The molecular structure of **5** is shown in Figure 1; selected bond distances and angles are collected in Table 5. The cluster contains a triangular array of osmium atoms, a terminal phosphonium acetylide ligand σ -bonded to Os(1), and an equatorial phosphine ligand coordinated to Os(2). Both Os(1) and Os(2) atoms are associated with three terminal carbonyls, while Os(3) is linked to four carbonyl ligands. The two osmium atoms Os(1)–Os(2) are bridged by a hydride. This explains the elongation of the Os(1)–Os(2) distance (3.051(1) Å) relative to the Os–Os bond length of 2.87 Å in $\text{Os}_3(\text{CO})_{12}$.^{14,15} Furthermore, the presence of the hydride causes some distortions in the equatorial plane of **5**: the angles C(2)–Os(1)–Os(2) = 114.0(4)° and P(1)–Os(2)–Os(1) = 115.40(8)° are greater than other angles in the equatorial plane of the cluster (94.9° on average). The acetylidyne ligand is linear (bond angles C(12)–C(11)–Os(1) = 173(1)° and C(13)–C(12)–C(11) = 179(1)°) and coordinated to Os(1) in an axial position (bond angles C(11)–Os(1)–Os(2) = 87.9(3)° and C(11)–Os(1)–Os(3) = 91.8(4)°). The C(11)–C(12) distance of 1.21(2) Å corresponds to a triple-bond length in uncoordinated acetylene. The Os(1)–C(11) σ -bond of 2.081(11) Å in **5** is similar to the analogous bond in **9** (2.075 Å)¹³ and

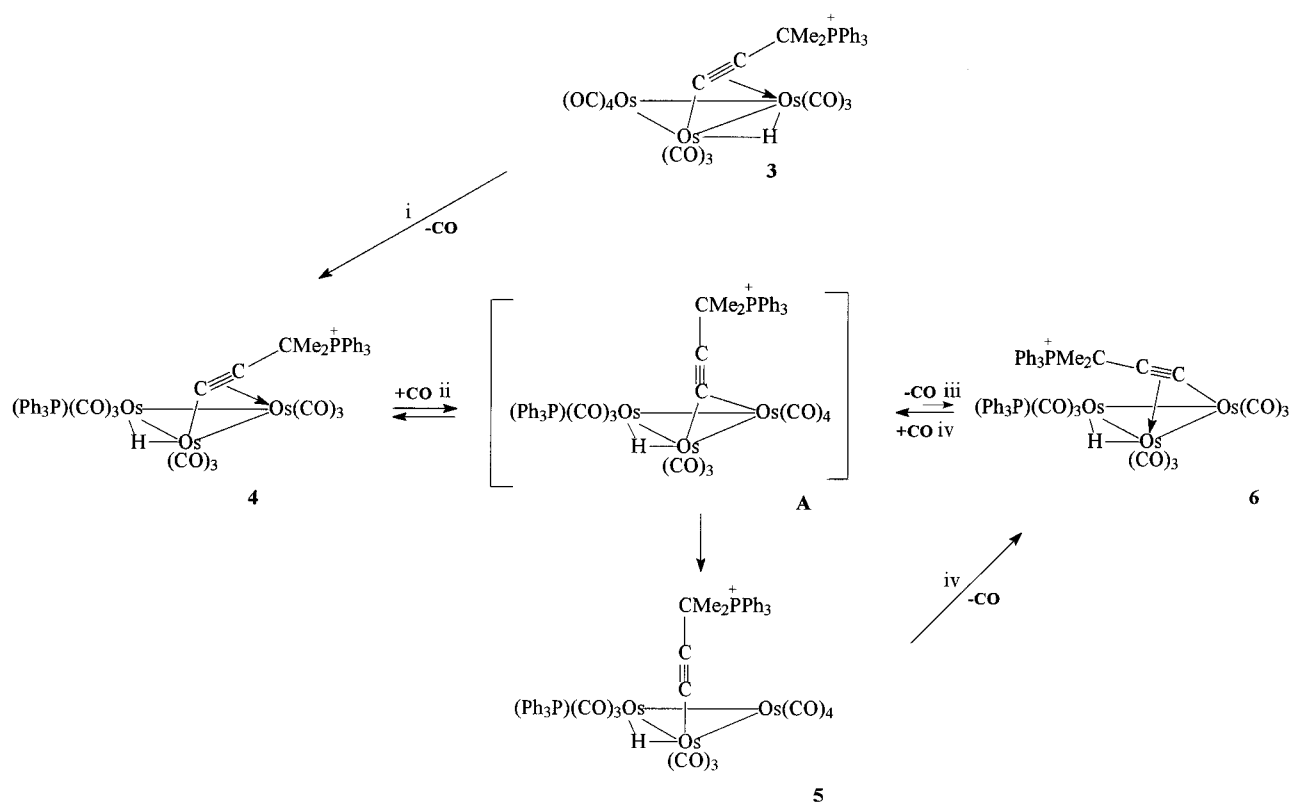
(13) Cherkas, A. A.; Taylor, N. J.; Carty, A. J. *J. Chem. Soc., Chem. Commun.* **1990**, 385

(14) Churchill, M. R.; De Boer, B. G. *Inorg. Chem.* **1977**, *16*, 878.

(15) Churchill, M. R.; De Boer, B. G.; Kofella, K. J. *Inorg. Chem.* **1976**, *15*, 1843.

Scheme 1^a

^a Reagents and conditions: (i) PPh_3 , $-78\text{ }^\circ\text{C}$; (ii) $-78\text{ }^\circ\text{C}$.

Scheme 2^a

^a Reagents and conditions: (i) PPh_3 ; (ii) $0\text{--}25\text{ }^\circ\text{C}$; (iii) $25\text{ }^\circ\text{C}$; (iv) $55\text{ }^\circ\text{C}$.

slightly longer than the $Os-C$ bond for a σ,π -coordinated acetylidy ligand (2.060 \AA in **9**¹³ and 2.066 \AA in $Os_3(\mu-H)(CO)_9(PMe_2Ph)(\mu-\sigma:\eta^2-C\equiv CPh)$ (**10**)¹⁶).

Decarbonylation of $[Os_3(\mu-H)(CO)_9(PPh_3)-(\sigma-C\equiv CCMe_2PPh_3)]BF_4$ (5**).** Cluster **5** is thermally quite stable, which might be due to a stabilizing effect of the phosphonium substituent in the acetylidy ligand. Only when **5** was kept in a CD_2Cl_2 solution at $25\text{ }^\circ\text{C}$ for 2 days was $5\text{--}10\%$ of a new compound formed, the ^1H

NMR spectrum of which showed a doublet for the hydride and two doublets for the nonequivalent Me groups. The ^{31}P spectrum of the product showed signals due to the phosphonium and phosphine phosphorus atoms (Table 2). We expected that this might be the product of decarbonylation of **5**, $[Os_3(\mu-H)(CO)_9(PPh_3)-(\mu-\sigma:\eta^2-C\equiv CCMe_2PPh_3)]BF_4$ (**6**) (Chart 2). Attempts to prepare **6** quantitatively were not successful; the best result was achieved by heating **5** in CD_3NO_2 at $55\text{ }^\circ\text{C}$ in a sealed tube for 15 h, resulting in an equimolar mixture of **5** and **6**. Our attempt to shift the equilibrium toward the formation of **6** (changing the temperature

(16) Koridze, A. A.; Kizas, O. A.; Petrovskii, P. V.; Kolobova, N. E.; Struchkov, Yu. T.; Yanovsky, A. I. *J. Organomet. Chem.* **1988**, 338, 81.

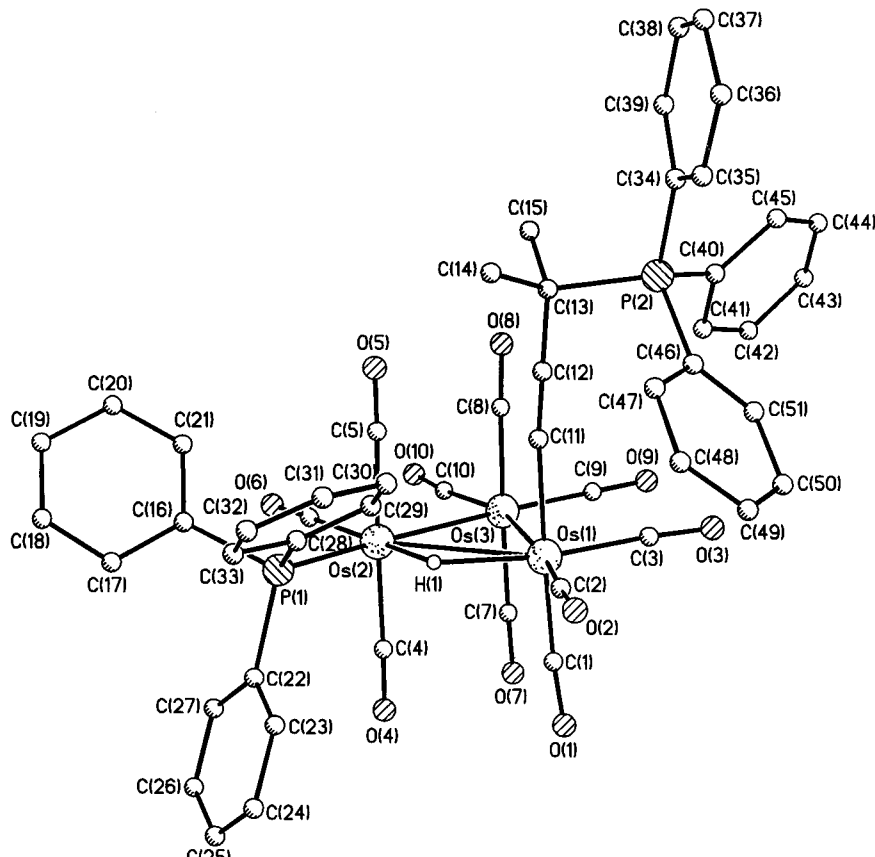


Figure 1. View of the cluster of $[\text{Os}_3(\mu\text{-H})(\text{CO})_{10}(\text{PPh}_3)(\sigma\text{-C}\equiv\text{CCMe}_2\text{PPh}_3)]\text{BF}_4$ (5).

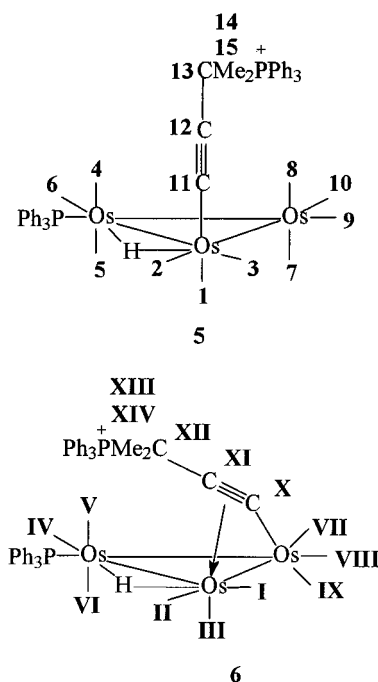
Table 5. Selected Bond Lengths (Å) and Angles (deg) in Complex 5

Os(1)–Os(2)	3.051(1)	Os(3)–C(9)	1.89(2)
Os(1)–Os(3)	2.892(1)	Os(3)–C(10)	1.90(2)
Os(2)–Os(3)	2.916(1)	P(1)–C(16)	1.83(1)
Os(1)–C(1)	1.88(1)	P(1)–C(22)	1.84(1)
Os(1)–C(2)	1.90(2)	P(1)–C(28)	1.82(1)
Os(1)–C(3)	1.90(2)	P(2)–C(34)	1.80(1)
Os(1)–C(11)	2.09(1)	P(2)–C(40)	1.79(1)
Os(2)–C(4)	1.95(1)	P(2)–C(46)	1.80(2)
Os(2)–C(5)	1.96(1)	P(2)–C(13)	1.88(1)
Os(2)–C(6)	1.91(2)	C(11)–C(12)	1.21(2)
Os(2)–P(1)	2.378(4)	C(12)–C(13)	1.46(2)
Os(3)–C(7)	1.91(2)	C(13)–C(14)	1.55(2)
Os(3)–C(8)	1.93(1)	C(13)–C(15)	1.48(2)
Os(3)–Os(1)–Os(2)	58.71(2)	C(12)–C(11)–Os(1)	173(1)
Os(3)–Os(2)–Os(1)	57.92(2)	C(11)–C(12)–C(13)	179(1)
Os(1)–Os(3)–Os(2)	63.36(2)	C(12)–C(13)–C(15)	114(1)
C(11)–Os(1)–Os(2)	87.9(3)	C(12)–C(13)–C(14)	112(1)
C(11)–Os(1)–Os(3)	91.8(4)	C(15)–C(13)–C(14)	109(1)
P(1)–Os(2)–Os(3)	173.25(8)	C(12)–C(13)–P(2)	105(1)
P(1)–Os(2)–Os(1)	115.40(8)	C(15)–C(13)–P(2)	109(1)
		C(14)–C(13)–P(2)	109(1)

and duration, reevacuation of the tube) were not successful.

The ^{13}C NMR spectrum of **6** (Table 4) fits the system in which the σ,π -phosphonium acetylide ligand is coordinated to the phosphine-substituted cluster. In the carbonyl region the spectrum displays nine resonances for the terminal carbonyls. The low-field signals V and VI with the largest $J_{\text{P}-\text{H}}$ couplings are due to the axial ligands of the $\text{Os}(\text{CO})_3\text{PPh}_3$ fragment. Signal IV with relatively large $J_{\text{P}-\text{H}}$ and $J_{\text{C}-\text{H}}$ couplings is due to the equatorial CO ligand of this fragment arranged trans to the hydride. On the basis of the $J_{\text{C}-\text{H}}$ value signal I can be assigned to the equatorial CO group of the $\text{Os}(\text{CO})_3(\mu\text{-H})$ unit, which is also trans to the hydride ligand. The two signals II and III show weak hydride couplings and are assigned to the same unit. Signals VII, VIII, and IX are weakly coupled to the phosphorus nucleus and not coupled to the hydride. They are assigned to the remaining $\text{Os}(\text{CO})_3$ unit, VIII to belonging the equatorial ligand of this moiety (*trans* to PPh_3) and the lowest field signal IX belonging to the axial

Chart 2



$\text{CO})_3(\mu\text{-H})$ unit, which is also trans to the hydride ligand. The two signals II and III show weak hydride couplings and are assigned to the same unit. Signals VII, VIII, and IX are weakly coupled to the phosphorus nucleus and not coupled to the hydride. They are assigned to the remaining $\text{Os}(\text{CO})_3$ unit, VIII to belonging the equatorial ligand of this moiety (*trans* to PPh_3) and the lowest field signal IX belonging to the axial

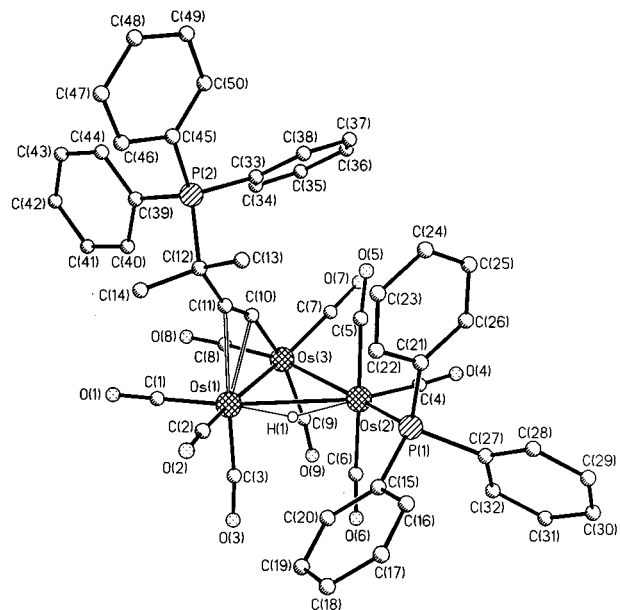


Figure 2. View of the cluster of $[\text{Os}_3(\mu\text{-H})(\text{CO})_9(\text{PPh}_3)(\mu\text{-}\sigma\text{:}\eta^2\text{-C}\equiv\text{CCMe}_2\text{PPh}_3)]\text{BF}_4$ (**6**).

ligand. Signals due to the hydrocarbon ligand have regular chemical shifts; however, there are some differences between the ^{13}C NMR spectra of **3** and **6**. For **3** the C_α and C_β atoms appear as a singlet and a doublet, respectively, whereas for **6** the pattern is reversed. Moreover, in the ^1H NMR spectra the signal due to the hydride ligand for **6** is shifted 2 ppm as compared to that for **3**. This allows us to conclude that **6** could be an acetylidyne cluster in which the hydride and acetylidyne ligands are located at different edges of the osmium triangle (Chart 2). This was confirmed by an X-ray analysis.

Crystal Structure of $[\text{Os}_3(\mu\text{-H})(\text{CO})_9(\text{PPh}_3)(\mu\text{-}\sigma\text{:}\eta^2\text{-C}\equiv\text{CCMe}_2\text{PPh}_3)]\text{BF}_4$ (6**)**. One of the two independent molecules of complex **6** is shown in Figure 2; selected bond distances and angles are collected in Table 6. The cluster is composed of a triangular array of osmium atoms and a bridging phosphonium acetylidyne ligand which is σ -bonded to Os(3) and π -bonded to Os(1). The phosphine ligand coordinates to Os(2) in an equatorial position. Each osmium atom is bound to three terminal carbonyl ligands. The bridging hydride ligand is located on the Os(1)–Os(2) edge. This explains the elongated Os(1)–Os(2) distance of 3.099 Å and increased bond angles C(2)–Os(1)–Os(2) and P(1)–Os(2)–Os(1) of 110.4 and 112.1°, respectively.

The π -coordination of the acetylene fragment with the Os(1) atom is asymmetrical in **6** (Os(1)–C(10) and Os(1)–C(11) bond lengths are 2.28 and 2.36 Å); this is similar to the bonding situation reported for **10**.¹⁶ The side-on coordination by the Os cluster in **6** leads to a more pronounced distortion of the acetylene fragment, which is reflected not only in the slight elongation of the triple C(10)–C(11) bond up to 1.28 Å (average) relative to the corresponding bonds in **10** (1.23 Å)¹⁶ and **9** (1.25 Å)¹³ but also in a decrease of the C(11)–C(10)–Os(3) and C(10)–C(11)–C(12) angles (158, 157° and 167, 164° in **6** and **10**, respectively).

Thus, we have found that the interaction of cluster **3** with PPh₃ yields the linear σ complex **5**; this interaction proceeds via the complex **4**. When the reaction mixture

is kept at 0 °C for 4 days, the following pattern is observed in the ^1H and ^{31}P NMR spectra: after 24 h the solution contains **3**, **4**, and **5** in a ratio of 5:2:4, and then the concentration of **3** decreases and that of **5** increases. The concentration of **4** remains constant until there is a noticeable amount of **3** in the solution (**3** > **4**), and then the concentrations of both **3** and **4** decrease. Clusters **3** and **4** disappear simultaneously, and the spectra show the presence of only **5** in solution. The ^1H and ^{31}P NMR spectra for **4** and **6** are very similar and differ only slightly in chemical shift values; it might be suspected that **4** and **6** are isomers. Unfortunately, complex **4** could not be isolated and crystallized for an X-ray analysis. The NMR data suggest the following route for its transformation into **5** and further into **6** (Scheme 2): the phosphine attacks **3**, replacing a CO in the Os(CO)₄ moiety to generate **4**, for which the barrier to $\sigma, \pi \leftrightarrow \pi, \sigma$ fluctuation might be relatively high^{11,12,17} and the interexchange is so slow that we can observe the formation of the individual isomer **4** in the spectra. The isomerization of **4** into **6** due to this rearrangement (Scheme 2) may involve the formation of an intermediate (**A**) in which the acetylidyne is a bridging one-electron ligand bound to the cluster in a $\mu\text{-}\eta^1$ fashion. An example of a ruthenium cluster with this type of bonding of the acetylidyne ligand has been reported.¹⁸ Then, the intermediate **A** can either transform to **6** or isomerize to **5**. The second route appears to be more preferable, and cluster **5** is the only product observed at 0 °C. At room temperature, **5** and **6** are formed in a 9:1 ratio. It should be noted that the transformations **3** → **4** → **5** proceed cleanly only in a sealed NMR tube. Running the reaction in an open system, especially under an argon stream, leads to decomposition products and to a sharp decrease in the yield of **5**. Therefore, it appears that the transformation **4** → **5** requires CO, which is liberated and accumulated in the NMR tube upon formation of **4** from **3**.

Complex **5** decarbonylates on heating to form **6**. The presence of CO is necessary for this reaction because and if it is carried out in an open system, only decomposition products are obtained as well as in the case of the transformation **4** → **5**. This reaction is reversible because the decarbonylation of **5** cannot be brought to completion and the highest yield of **6** is 50%. The peculiarities of the reactions presented in Scheme 2 led us to the conclusion that not only the transformation **5** → **6** takes place but also the transformation **6** → **5** due to $\sigma, \pi \rightarrow \pi, \sigma$ exchange¹⁹ also occurs; the reaction proceeds via **A**, which further transforms to **6** again.

The ^1H NMR spectrum of a mixture **5** and **6** (Figure 3) supports this conclusion. When the temperature is raised, the signals for the Me groups of cluster **6** broaden and the distance between these signals decreases. This temperature dependence can be associated with the $\sigma, \pi \rightarrow \pi, \sigma$ interconversion during **6** → **5** transformation via **A** rather than with the exchange of the hydride ligand, because the latter shows a double set of satellite signals

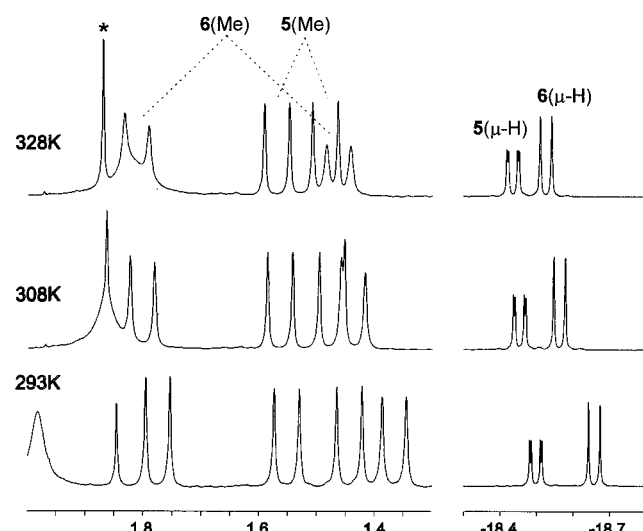
(17) Broun, S. R.; Evans, J. *J. Chem. Soc., Dalton Trans.* **1982**, 1049.

(18) Carty, A. J.; Taylor, N. J.; Smith, W. E. *J. Chem. Soc., Chem. Commun.* **1979**, 750.

(19) We had in mind that the ligand exchange is the driving force for all these transformations; however, this process is broken by the formation of cluster **5** and the necessity of its decarbonylation.

Table 6. Selected Bond Lengths (Å) and Angles (deg) in Complex 6 (for the Two Independent Molecules A and B)

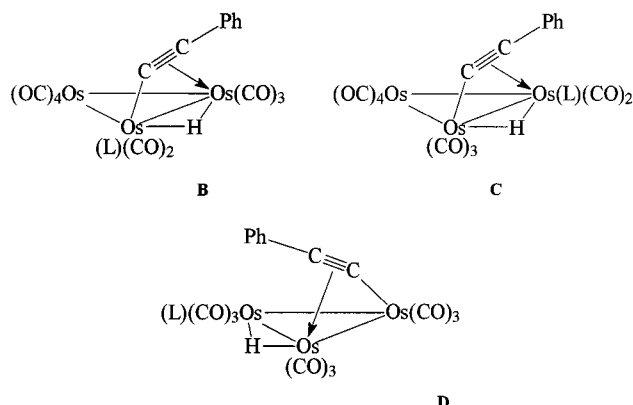
	A	B	A	B
Os(1)–Os(2)	3.100(1)	3.097(1)	Os(3)–C(9)	1.90(2)
Os(1)–Os(3)	2.785(1)	2.782(1)	Os(3)–C(10)	2.03(2)
Os(2)–Os(3)	2.865(1)	2.864(1)	P(1)–C(15)	1.815(8)
Os(1)–C(1)	1.86(2)	1.89(2)	P(1)–C(21)	1.830(9)
Os(1)–C(2)	1.94(2)	1.92(2)	P(1)–C(27)	1.836(8)
Os(1)–C(3)	1.88(2)	1.91(2)	P(2)–C(33)	1.797(9)
Os(1)–C(10)	2.28(2)	2.29(2)	P(2)–C(39)	1.791(9)
Os(1)–C(11)	2.35(2)	2.37(2)	P(2)–C(45)	1.79(1)
Os(2)–C(4)	1.86(2)	1.89(2)	P(2)–C(12)	1.90(2)
Os(2)–C(5)	1.96(2)	1.97(2)	C(10)–C(11)	1.24(2)
Os(2)–C(6)	1.92(2)	1.88(2)	C(11)–C(12)	1.50(2)
Os(2)–P(1)	2.364(4)	2.366(4)	C(12)–C(13)	1.53(2)
Os(3)–C(7)	1.90(2)	1.90(2)	C(12)–C(14)	1.48(2)
Os(3)–C(8)	1.84(2)	1.87(2)		1.54(2)
Os(3)–Os(1)–Os(2)	57.98(3)	58.02(3)	C(11)–C(10)–Os(3)	158(1)
Os(3)–Os(2)–Os(1)	55.49(2)	55.48(2)	C(11)–C(10)–Os(1)	78(1)
Os(1)–Os(3)–Os(2)	66.53(3)	66.50(3)	Os(3)–C(10)–Os(1)	80.2(5)
C(10)–Os(1)–Os(3)	46.0(5)	45.1(4)	C(10)–C(11)–C(12)	156(2)
C(11)–Os(1)–Os(3)	77.0(4)	77.7(4)	C(11)–C(12)–C(13)	112(1)
C(10)–Os(1)–Os(2)	73.2(4)	74.3(4)	C(14)–C(12)–C(11)	112(2)
C(11)–Os(1)–Os(2)	90.5(4)	91.2(4)	C(14)–C(12)–C(13)	111(2)
P(1)–Os(2)–Os(3)	165.3(1)	165.0(1)	C(14)–C(12)–P(2)	110(1)
P(1)–Os(2)–Os(1)	112.0(1)	112.1(1)	C(11)–C(12)–P(2)	104(1)
C(10)–Os(3)–Os(1)	53.7(4)	54.2(5)	C(13)–C(12)–P(2)	107(1)
C(10)–Os(3)–Os(2)	81.9(4)	83.9(4)		108(1)

**Figure 3.** Variable-temperature ^1H NMR spectra (δ , ppm) of the two clusters **5** and **6**. The asterisk denotes a peak due to MeNO_2 .

(asymmetric structure) and the $J_{^{187}\text{Os}-^1\text{H}}$ values 45.44 and 41.84¹¹ correspond to stereochemically rigid hydride bridges.

Thus, the isomerization of **4** into **6** shown in Scheme 2 might occur by two routes: either with the participation of the intermediate complex **A** (the presence of CO is necessary for the **4** \rightarrow **5** and **5** \leftrightarrow **6** stages) at 25 °C or with the participation of complex **5**, which is formed at 0 °C and decarbonylates at 55 °C to yield **6**.

The results presented in this paper allow us to reconsider the structure of the isomeric complexes $\text{Os}_3(\mu\text{-H})(\text{CO})_9(\text{PMe}_2\text{Ph})(\mu\text{-}\sigma\text{:}\eta^2\text{-C}\equiv\text{CPh})$,¹¹ for which the structures **B** and **C** were proposed (Figure 4). The structure **B** was determined by X-ray crystallography, whereas the structure **C** was proposed on the basis of

**Figure 4.** Isomers of the cluster $[\text{Os}_3(\mu\text{-H})(\text{CO})_9(\text{PMe}_2\text{Ph})(\mu\text{-}\sigma\text{:}\eta^2\text{-C}\equiv\text{CPh})]$ ($\text{L} = \text{PMe}_2\text{Ph}$).

the ^1H and ^{31}P NMR spectra. We believe now that, for the second isomer, the structure **D** is more likely. The chemical shift $\delta = -18.72$ and $J_{\text{H}-\text{P}} = 13.3$ Hz for the hydride signal are very similar to those for **6** (Table 1), in which the hydride and acetylidy bridges are located at different edges of the osmium triangle.

Acknowledgment. This work was financially supported by grants from the Russian Foundation for Basic Research (Project Nos. 00-03-32861 and 00-03-32807) and INTAS (Project No. 97-3199).

Supporting Information Available: Tables of atomic coordinates, bond lengths, and angles, views of clusters **5** and **6** with the representation of atoms by thermal ellipsoids ($p = 50\%$), and tables of anisotropic thermal parameters. This material is available free of charge via the Internet at <http://pubs.acs.org>.